# First insights into the binding mechanism and colour effect of the interaction of grape seed 11S globulin with malvidin 3-glucoside by fluorescence spectroscopy, differential colorimetry and molecular modelling

Francisco Chamizo-González[1], Ignacio García Estevez[2], Belén Gordillo[1*], Elvira Manjón[2], M.T. Escribano-Bailón[2], Francisco J. Heredia[1], and M. Lourdes González-Miret[1].

[1]Food Colour & Quality Lab., Área de Nutrición y Bromatología. Facultad de Farmacia. Universidad de Sevilla. 41012-Sevilla, Spain

[2]Grupo de Investigación en Polifenoles, Facultad de Farmacia, Universidad de Salamanca, Campus Miguel de Unamuno, E 37007 Salamanca, Spain

Francisco Chamizo-González: fchamizo@us.es

Ignacio García-Estévez: igarest@usal.es

Belén Gordillo: bgordillo@us.es

Elvira Manjón: elvira87@usal.es

M.T. Escribano-Bailón: escriban@usal.es

Francisco J. Heredia: heredia@us.es

M. Lourdes Gonzalez-Miret: miret@us.es

* Corresponding author: Belén Gordillo

Belén Gordillo

Food Colour & Quality Lab., Área de Nutrición y Bromatología. Facultad de Farmacia. Universidad de Sevilla. 41012-Sevilla, Spain

Tel.: +34 9556760

e-mail: bgordillo@us.es

## ABSTRACT

Recently, the search for alternative proteins endogenous to grapes to be used as wine colour protecting agents became an important research trend. In this study, the molecular interaction between the grape seed 11S globulin from winemaking by-product and malvidin 3-glucoside was investigated by fluorescence, differential colorimetry and molecular modelling. Fluorescence studies revealed the formation of grape seed protein-pigment complex whose $K_S$ was $8.5x10^4$ $M^{-1}$ and binding sites, n=1.3. Malvidin 3-glucoside showed darker and more vivid bluish colour of in the presence of 11S globulin, suggesting the flavylium cation protection in a hydrophobic region of the protein. Docking analysis and molecular dynamics simulation indicated that malvidin 3-glucoside interacts mainly with the acidic subunit (40 kDa) of the 11S globulin monomer (60 kDa). An average of two hydrogen bonds and Van der Wall forces were the main interaction forces found for the protein-pigment complex, whose stability was confirmed by root-means-square deviation.



**Keywords**: grape seed 11S globulin; winemaking by-product; malvidin 3-glucoside; colour; fluorescence quenching; guided docking.

## 1. INTRODUCTION

Anthocyanins are natural flavonoid pigments responsible for orange-red to purple-blue colours in many fruits, vegetables, and derived food products such as wines (Delgado-Vargas, Jiménez, & Paredes-López, 2000). As potent antioxidants, anthocyanins are of great interest for the food industry not only because they impact the sensory quality of foods but also for their multiple health benefits associated with their consumption in the diet (He & Giusti, 2010).

In red wines, anthocyanins are the 3-O-monoglucosides of five major anthocyanidins (delphinidin 3-glucoside, cyanidin 3-glucoside, peonidin 3-glucoside, petunidin 3-glucoside, and malvidin 3-glucoside) with malvidin 3-glucoside (mv3glc) and their derivatives by far the most abundant pigments contributing for colour (Trouillas et al., 2016). The basic chromophore structure of anthocyanins consists in a flavylium cation that shows a vivid red coloration in very acidic solutions (pH≤1). However, at moderately acid pH values, as those found in wines (3.5-4.2), the flavylium cation is relatively instable and very susceptible to decolouration and degradation against several factors (Pina, Oliveira, & de Freitas, 2015). In wines, its colour stability is affected by pH, anthocyanin chemical structure and concentration, exposure to temperature, oxygen, light, enzymes, and other wine components or additives such as ascorbic acid, sugars, or sulphites, among others (Escribano-Bailón, Rivas-Gonzalo, & García-Estévez, 2019). In this regard, many winemaking techniques and oenological strategies have been developed to preserve the anthocyanin stability and colour (Sacchi, Linda, Bisson, Douglas, & Adams, 2005; Soto Vázquez, Río Segade & Orriols Fernández, 2010). Moreover, natural pigment-stabilizing mechanisms exist in wines that protect the coloured flavyliym cation from the nucleophilic attack of water, pH changes, and decolouring agents; mainly copigmentation interactions, but also certain associations with biopolymers including

polysaccharides or proteins (Boulton, 2001; Escribano-Bailón & Santos-Buelga, 2012; Trouillas et al., 2016; Fernandes et al., 2021).

Over the last years, the researches on interactions between wine pigments and plant proteins have been steadily increasing. This recent approach has provided valuable information on the protection of anthocyanins through the interactions with different protein types contributing to promote their application in the wine industry (Granato, Ferranti, Iametti, & Bonomi, 2018; Marangon Vincenzi & Curione, 2019; Gordillo, Chamizo-González, Gonzalez-Miret, & Herdia, 2021).

Plant seed-storage proteins include albumins, globulins, gliadins and glutenins fractions of which globulins comprise one the major fraction. Currently, some studies have shown that globulins from different vegetal sources present good functional properties to protect the stability and antioxidant activity of anthocyanin pigments. Li et al. (2020) assessed the complexation characteristics between different rice protein (RP) fractions and black rice anthocyanins (ACN) by fluorescence spectroscopy at pH 3. This study concluded that globulin-ACN complexes stablished strong binding interaction involving the flavylium cation, with quenching constants larger than albumin-ACN complexes due to the more hydrophobic areas of globulins. As well, the globulin-ACN complexes exhibited greater DPPH (1,1-diphenyl-2-pycrylhydrazyl) and ABTS (2,2-azino-bis 3-ethylbenzothiazoline-6-sulfonic acid) radical scavenging in comparison to RP albumin, prolamin and glutelin due to the more flexible and unfolded structure of globulins resulting in a better capability to react with the free radicals. On the other hand, Ren, Xion, & Li (2019) compared the non-covalent binding mechanisms between cyanidin-3-O-glucoside and two main soy protein fractions: β-conglycinin (7S) and glycinin (11S) at pH 3, confirming the formation of spontaneous complexation processes between globulins and the flavylium cation driven by electrostatic forces. In comparison, cyanidin

3-glucoside showed a stronger binding affinity toward 11S globulin owing to more positive charges of 11S than 7S. Similarly, 7S and 11S globulins from soybean have also demonstrated a protective effect on the stability of cyanidin 3-glucoside and to improve its antioxidant capacity in simulated digestions. Again, the effects were stronger with the 11S globulin (Zheng, Zheng, Zhao, Yi, & Shengbao, 2021).

Of special interest for the wine industry are proteins endogenous to grape like those obtained from grape seed wine by-products, which have been proposed as a sustainable alternative to the use of other biopolymers subjected to more legal restrictions (i.e. animal origin and synthetics) (Baca-Bocanegra, Nogales-Bueno, Hernández-Hierro, & Heredia, 2021; Gordillo et al., 2021; Mora-Garrido, Cejudo-Bastante, Heredia, & Escudero-Gilete, 2022). At this respect, the 3D structure of 7S and 11S globulins from *Vitis vinifera* L. grape seed have been elucidated for the first time in our previous studies by combining proteomic and computational techniques (Chamizo-González, Gordillo, & Heredia, 2021; Chamizo-González, Heredia, Rodríguez-Pulido, González-Miret, & Gordillo, 2022). In addition, we have confirmed by means of theoretical studies that both 7S and 11S grape seed globulins could stablish different types of interactions (hydrogen bonding, alkyl and π-π) with the main grape anthocyanin (mv3glc). However, such as interactions has been scarcely studied and very little is still known concerning the real effect on the colour of wine anthocyanins. Although a basic molecular interaction mechanism similar to copigmentation has been suggested, many questions and experimental evidence remain unclarified for the promising functionality of grape seed globulins.

Thus, this work aims to provide an improved understanding of the binding mechanism of the interaction between the major grape seed storage protein (11S globulin, 11SGb) and the major wine pigment (mv3glc) in relation to the effect on the anthocyanin colour. For this purpose, fluorescence quenching in combination with colorimetric studies were

carried out in model solution to provide experimental evidence and fundamental information about the molecular interaction (affinity constant and the stoichiometry of the complex) as well as the potential colour effect. Complementary, molecular modelling studies based on directed docking techniques were developed to assess the specific binding site and the interaction forces of the protein-anthocyanin complex. This study is expected to contribute to the potential use of plant proteins endogenous to grape as potential colour protecting agents in wines.

## 2. MATERIAL AND METHODS

### 2.1. Reagents

Malvidin 3-glucoside (≥97 %) and Bovine Serum Albumin (BSA, ≥98 %) were purchased from Extrasynthese (Genay, France). SDS-PAGE (sodium dodecyl sulphate-polyacrylamide gel electrophoresis) reagents (Tris-HCl, dithiothreitol: SDS, bromophenol blue, β-mercaptoethanol, glycerol, acrylamide, and bisacrylamide) were purchased from Sigma-Aldrich (Steinheim, Germany). All other chemicals (ethanol, citric acid, sodium citrate, sodium chloride, and trizma hydrochloride) were of analytical grade and supplied by Panreac Química (Barcelona, Spain).

### 2.2. Extraction of grape seed globulins and purification

Seed globulins were extracted from defatted grape seed flour (industrial wine by-product) supplied by ALVINESA Natural Ingredients, S.A. (Daimiel, Ciudad Real, Spain), following the previously described method by Chamizo-González, et al. (2022) with slight modifications. Globulin fraction (salt soluble) was extracted with 0.5 M Sodium chloride (1:10 w/v) with constant stirring for 1 h at room temperature (25±0.2 °C). The obtained salt soluble fraction was centrifuged (8000 g for 10 min) and the flour residue was submitted to the same process twice (each stirring for 30 min). The three supernatants were combined, filtered through 0.45 μm nylon, and dialyzed during 48 h at 4 °C against

ultrapure water using a Spectra/Por® 1 regenerated cellulose dialysis membrane 6-8 kDa (Spectrum™ Labs.com Europe).

The globulin extract obtained (mainly comprised by 11SGb) was freeze-dried (lyophilizer Cryodos-80, Telstar Varian DS 102) and stored at -20 °C for further analysis.

**2.3. SDS-PAGE analysis of grape seed globulins and quantification of protein subunits by image densitometry**

The molecular weight and subunit composition of the grape seed globulin extract was analysed under reducing conditions by SDS-PAGE using the Mini-Protean® 3 system (BioRad, Hercules, CA, USA). Four replicates of the SDS-PAGE analysis were carried out as follows: 10 mg of lyophilized protein extract was dissolved in 1 ml of distilled water. Then, 150 µl of the aqueous protein extract was mixed with 50 µl of 0.02 M Tris-HCl loading buffer pH 6.8 (containing glycerol 40% w/v, SDS 5% w/v, β-mercaptoethanol 20%, and 0.01% Bromophenol Blue). Protein samples were then denatured at 100 ˚C for 5 min. Samples (15 µl) were loaded into 14% polyacrylamide gel 1.5 mm (acrylamide: bisacrylamide, 29:1) and electrophoresis was run at constant voltage (170 V) for 50-60 min. Proteins were visualized after incubation with Coomassie staining solution (40% v/v ethanol, 10% v/v acetic acid, 50% distilled water and 0.01 % Coomassie blue R-250 w/v). Subsequently, the gels were decolorized in a solution of 40% v/v ethanol and 10% v/v acetic acid while stirring until the bands were adequately visualized. The standard molecular weight proteins (ranging from 20 to 200 kDa) used were the PageRuler ™ unstained protein ladder (Thermo Fisher Scientific Inc., Vilnius, Lithuania).

For quantification of 11SGb fraction and their respective subunits the protein bands were analysed by image densitometry as described for other plant proteins (Mujoo, Trinh, & Perry, 2003), using the software GelAnalyzer 2010a (www.GelAnalyzer.com). Gel

replicates (n=4) were scanned and the images were digitized and stored until needed for quantitative analysis. The software GelAnalyzer 2010a allows display, store, and analyse electrophoretic patterns covering all the main aspects of gel evaluation from automatic lane detection to background subtraction methods, and calibration. A solution of commercial standard BSA (1 mg/ml) was used as a protein standard for quantification purposes. BSA solutions at increasing concentration (12.5, 25, 50, 100, and 200 µg/ml) was loaded into each gel to obtain a calibration curve to quantify (µg) the different globulin subunits. The proportions (%) of each globulin subunit relative to the sum of the total subunits identified in the respective gel lane were also calculated.

### 2.4. Fluorescence quenching

The interaction between grape seed globulins and mv3glc was investigated using fluorescence quenching measurements. The intrinsic fluorescence of proteins is due to the presence of aromatic amino acids phenylalanine, tyrosine and tryptophan, the latter being predominant in proteins (Lakowicz, 2013). Intrinsic fluorescence of samples was carried out using a fluorescence spectrophotometer Perkin-Elmer LS 55 (Waltham, MA, USA) in 1-cm quartz cuvettes at controlled temperature (25 °C ± 0.1). In all experiments, proteins and mv3glc stocks solutions were prepared in 0.2 M citrate buffer (pH 3.5) with the ionic strength adjusted with 0.5 M sodium chloride. The mixtures (final volume of 2 ml) were prepared at constant protein concentration (50 µM, mainly comprised of 11SGb) and increasing concentrations of mv3glc (0-100 µM). The assay was performed in triplicate. After mixing, the samples were transferred to the fluorimeter cell and the emission spectra were measured. The excitation wavelength was 280 nm and the emission spectrum was recorded between 290 and 450 nm. The excitation and emission slit widths were both 5.5 nm, the scanning speed was 1200 nm/min, and the voltage was 700 v. After each measurement, the cell was washed with ethanol and distilled water.

The fluorescence quenching constants were analysed by the Stern-Volmer equation (1) (Wei et al., 2018).

$$\frac{F_0}{F} = 1 + K_{SV}\, x\, [Q] = 1 + K_q x\, \tau_0\, x\, [Q] \qquad (1)$$

where, $F_0$ and F were the fluorescence intensities of proteins before and after the addition of the quencher, $[Q]$ is the molar concentration of mv3glc; $K_{SV}$ is the Stern-Volmer quenching constant; $K_q$ is the bimolecular quenching rate constant; and $\tau_0$ is the lifetime of the fluorophore in the absence of quencher ($10^{-8}$ s) (Wei et al., 2018).

From the following equation (2) it is possible to calculate $K_q$ (Rawel, Meidtner, & Kroll, 2005).

$$K_q = \frac{K_{sv}}{\tau_0} \qquad (2)$$

When $K_q$ is greater than the diffusion-limited maximum extinction constant in water ($2x10^{10}$ $M^{-1}$ $s^{-1}$) indicates that static, and not dynamic, quenching was the main quenching mechanism (Casanova et al., 2018). In this circumstance the Stern-Volmer Eq.(1) is modified to the double logarithmic Stern-Volmer Eq. (3), where $K_S$ represents the "static quenching constant" (Lakowicz, 2013):

$$log\ \frac{(F_0 - F)}{F} = log K_S + n log[Q] \qquad (3)$$

Thus, for the static extinction mechanism, the number of binding sites *n* and the static quenching constant $K_S$ can also be determined by linear regression from a plot of log ($F_0$-F/F) as a function of [Q]. The slope of the double logarithmic Stern-Volmer Eq. (3) represents the number of binding sites *n* and the intersection represents the binding constant.

## 2.5. Colour analysis by differential tristimulus colorimetry

The effect of grape seed globulins on the colour of mv3glc was assessed in model solutions prepared in 0.2 M citrate buffer (12% ethanol at pH 3.5) with the ionic strength adjusted with 0.5 M sodium chloride. Mixtures of anthocyanin/protein solutions were prepared by adding aliquots of 11SGb extracts (10 mg/ml) to mv3gl solutions ($10^{-4}$ M) at three protein concentration levels (1.5, 2.5 and 5 mg/ml). A solution of mv3glc at the same concentration without protein addition was prepared as control sample. All solutions were prepared in triplicate (n=12), stored closed in darkness at 25 °C and left to equilibrate for 30 min before spectroscopic measurements.

The absorption spectra (380-770 nm) of samples were recorded at constant intervals ($\Delta\lambda$ =2 nm) with a plate reader spectrophotometer (Synergy HTX, Bio-Tek, Winooski, VT). The absorbance spectra of mv3glc solutions were corrected in the visible range by the absorbance spectra of 11SGb solutions at increasing concentrations to avoid any interference in the measurement of the colour effect of grape seed proteins. CIELAB parameters were calculated from the absorption spectra by using the original software CromaLab© (Heredia; Álvarez; González-Miret; & Ramírez, 2004) following the recommendations of the Commission International de L'Eclariage: the CIE 1964 10° Standard Observer and the Standard Illuminant D65 (CIE, 2004). CIELAB parameters calculated were: L* (the correlate of lightness; ranging from 0, black, to 100, white), and two colour coordinates, a* (which takes positive values for reddish colours and negative values for greenish ones) and b* (positive for yellowish colours and negative for the bluish ones). From the a* and b* coordinates, other colour parameters are defined: the hue angle ($h_{ab}$, the correlate of chromatic tonality), and the chroma ($C^*_{ab}$, the correlate of saturation).

The colour variations induced by grape seed globulins on mv3gcl colour was assessed by Differential Tristimulus Colorimetry according to the methodology described in Gordillo, et al. (2015), which is based on the application of diverse colour difference formulas by using the scalar (L*, a*, b*) and cylindrical (L*, $C^*_{ab}$, $h_{ab}$) CIELAB colour parameters. First, colour-differences between mv3glc solutions and the same solutions containing increasing concentrations of grape seed 11SGb (1.5, 2.5, and 5.0 mg/ml) was calculated by applying the CIE76 colour difference formulae: $\Delta E^*_{ab} = [(\Delta L^*)^2 + (\Delta a^*)^2 + (\Delta b^*)^2]^{1/2}$. Moreover, the colour difference ($\Delta E^*_{ab}$) calculated between each solution (L*, a* and b*) with respect to distilled water (L*=100, a*=0, b*=0; as an achromatic reference) was referred as its "Total Colour" (named $E= [(L^*-100)^2 + (a^*-0)^2 + (b^*-0)^2]^{1/2}$). In this way, the Total Colour (E) of mv3glc solutions in absence and presence of grape seed 11SGb were compared.

In order to assess the trend of the colour changes in mvglc solutions due to the effect of grape seed 11SGb, the absolute lightness, chroma and hue difference was calculated by pair of samples ($\Delta L^*$, $\Delta C^*_{ab}$, $\Delta h_{ab}$). Also, the weight of the three- colour attributes for a given colour difference was calculated as the relative contribution of the lightness, chroma, and hue that make up the colour difference parameter ($\Delta E^*_{ab}$), as follows:

- Relative contribution (%) of lightness: $\%\Delta L=[(\Delta L^*)^2 / (\Delta E^*_{ab})^2] \times 100$

- Relative contribution (%) of chroma: $\%\Delta C=[(\Delta C^*_{ab})^2 /(\Delta E^*_{ab})^2]\times 100$

- Relative contribution (%) of hue: $\%\Delta H=[(\Delta H)^2/(\Delta E^*_{ab})^2]\times 100$,

being $\Delta H$ mathematically deduced from: $\Delta H=[ (\Delta E^*_{ab})^2- ((\Delta L)^2 + (\Delta C)^2 ) ]^{1/2}$

**2.6. Guided Docking study between grape seed 11SGb and mv3glc**

Guide docking refers to docking approaches that incorporate some degree of chemical information to actively guide the orientation of the ligand into the binding site (Fitzjohn & Bates, 2003). In our previous study (Chamizo et al., 2022), coupling assays using the

AutoDock Vina software allowed predicting the putative binding of mv3glc with two grape seed 11SGb (F6HZK2 and F6HZK3), recently identified for the first time. Their 3D structures were also satisfactory constructed, validated and energetically optimized by homology modelling by using UNIPROTKB database, the Mascot search engine software, the SWISS-MODEL tool from the EXPASY server, and the Gromacs 5.0.7 software. In this first coupling study, a grid box was designed for both F6HZK2 and F6HZK3 proteins to define possible ligand-protein binding interaction sites, whose dimensions were selected to cover the entire proteins. For F6HZK2 the box size selected was of 84×62×83 points and centred on the coordinate of X:-39.03, Y:9.61, Z:82.47; and for F6HZK3 the box size was of 81×79×73 points and centred on the coordinate of X:-65.28, Y:-8.21, Z:-24.84.

In this new computational study, the same docking methodology have been specifically targeted to the major hydrophobic region of the proteins previously identified in Chamizo et al., (2022), instead to the entire size protein. In this case, the coupling study was recalculated for the interaction between mv3glc and the F6HZK3 protein, which was the grape seed 11SGb with the best structural quality parameters obtained. For this purpose, the AutoDock Vina software (Trott & Olson, 2010) was used for the new coupling analysis, and a grid box with a specific size of 41×38×41 points was considered this time for the F6HZK3 protein, which was centred in this case at coordinates X: -40.6, Y: -7.16, Z: -29.04. With the Autodock tools all PDBQT files were generated to include the coordinates and partial charges of all atoms. For the protein structure, all hydrogen atoms were considered, partial atomic charges were calculated, water and ions were removed, and Kollman charges and polar hydrogens were added to the macromolecule since all these aspects are significantly involved in the ligand interaction. Other coupling parameters such as the energy range was considered equal to 3, the completeness equal

to 8 and the number of nodes equal to 9. On the other hand, the 2D and 3D chemical structures of mv3glc were modelled and optimized with the Avogadro software from the initial structure obtained in the PubChem data base, as described in Chamizo et al., (2022), considering the hydrogens in the structure at pH 3.5.

The positions of the protein atoms were kept fixed and the torsion angle of the glycosidic bond of the ligand was rotated until the rigid docking analysis allowed the favourable docking.

Different software was used to carry out the molecular modelling analysis. To visualize structures and analyse the results the UCSF Chimera software was used (Pettersen et al., 2004). 2D illustrations of the mv3glc sites interacting with the amino acids of the 11SGb F6HZK3 were made with Discovery Studio visualizer software.

**2.7. Molecular dynamics simulation of the 11SGb-mv3glc complex**

To assess the stability of the complex interaction (11SGb F6HZK3/mv3glc), molecular dynamics (MD) simulation were performed using Gromacs 5.07 software (https://manual.gromacs.org/) with the GROMOS force field. The topology file for mv3glc for each of the complexes was obtained from the CGenFF server (Vanommeslaeghe et al., 2010).

The protein-ligand complex was solvated in an explicit single point charge (SPC) water molecule box and simulated using periodic boundary conditions (PBC) and particle-mesh Ewald summation (PME) to enhance electrostatic interactions. The system power was minimized using 1000 steps. Two equilibration steps of 100 ps each were performed to reach the optimal pressure and temperature conditions. The reference pressure and temperature were 1 bar and 300 K (GROMACS 5.0.7 package). Once two equilibration phases were completed, the system was set to the desired temperature and pressure. Then, a 10 ns MD simulation was run with a 2-fs lics time step algorithm. Finally, the resulting

trajectory was analysed using GROMACS earnings. The root means square deviation parameter (RMSD) was used to calculate how much the position of the ligand varies relative to the protein during the simulation time. Moreover, the root mean square fluctuation (RMSF) and hydrogen bond were calculated by the GROMACS scripts.

### 2.8. Statistical analysis

Statistical analyses were performed using Statistica v.8.0 (Statsoft, 2007). Univariate analysis of variance (Tukey test, $p<0.05$.) was applied to establish statistical differences among samples.

## 3. RESULTS AND DISCUSSION

### 3.1. SDS-PAGE profile and quantification of the subunits of grape seed 11SGb

Electrophoretic patterns of the grape seed 11SGb fraction and their respective subunits analysed under reducing conditions is shown in Fig. 1. The globulin fractions extracted (n=4, lanes 7-10) showed similar patterns with two major polypeptide bands of about 40 and 20 kDa, which were slightly different regarding their relative amounts. These results agreed with those of our previous study (Chamizo-Gonzalez et al., 2022), in which the main monomer of the grape seed 11SGb had a molecular mass of 60 kDa (under non-reducing conditions) comprised by two subunits (an acidic one of ~40 kDa and a basic one ~20 kDa) linked by a disulphide bridge. However, the quantification of the 11SGb subunits was not assessed in our previous study, which can be of interest for technological purposes of such as proteins endogenous to grape in the wine industry. For this reason, the content (µg) and relative proportions (%) of the grape seed 11SGb subunits was analysed by SDS-PAGE coupled with image densitometry by using a linear calibration ($R^2$=0.950) with the BSA protein standard (Fig.1, lanes 1-5). Results for the content of the acidic subunit (40 kDa) was 2.15 ±0.25 µg and for the basic subunit (20 kDa) was 1.70 ± 0.12 µg, being these differences significant ($p<0.05$). The proportions for the acid

and basic subunits corresponded to 55.8 % and 44.2 % of the total content of the main 11SGb monomer (60 kDa), and hence, were similar to the proportions described for the same subunits of 11S storage proteins in different soybean varieties (Mujo et al., 2003).

### 3.2. Binding constants of the interaction between grape seed 11SGb and mv3glc by fluorescence quenching

In this study, the interaction between mv3glc and the grape seed 11SGb was assessed by fluorescence quenching, which has been widely used to study polyphenols-protein interactions providing useful information about the binding affinities on the complexes formed (Ferrer-Gallego et al., 2016). Fluorescence study was carried out in 0.2 M citrate buffer at pH 3.5 with the ionic strength adjusted with 0.5 M sodium chloride. Fig. 2A shows the mean fluorescence emission spectra (at $\lambda_{ex}$ 280 nm and 25 °C) of the grape seed 11SGb in the absence and presence of increasing concentrations of mv3glc (from 20 μM to 100 μM), after subtracting the corresponding blank assay for the same concentration of mv3glc. As observed, the fluorescence emission spectra of grape seed 11SGb ($\lambda_{max}$~346 nm) was gradually quenched upon increasing mv3glc concentration, suggesting grape anthocyanin binding the major grape seed proteins. After the addition of five-fold excess of the mv3glc (from 20 to 100 μM), the 11SGb fluorescence decreases from 9 % to 43 %, indicating that the quenching effect was notable and higher than those described by Casanova et al., (2018) for the interaction between cyanidin-3-O-glucoside and sodium caseinate (fluorescence decreases of 18 % at 40 μM of anthocyanin, pH=2).

Fluorescence quenching has two main mechanisms, generally divided into static and dynamic quenching. Static quenching results from collisional encounters between the fluorophore and the quencher, whereas dynamic quenching results from the formation of a ground-state complex between the fluorophore and the quencher (Casanova et al., 2018). Thus, to further understand the binding mechanism for the 11SGb and mv3glc, the

fluorescence data were analysed using the Stern-Volmer equations to determine the quenching constants of the interaction. The fluorescence changes induced by mv3gcl binding to the grape seed 11SGb are presented in Fig. 2B as the ratio $F_0/F$ versus the mv3glc concentration at the maximum emission wavelength, from which $K_{SV}$ and $K_q$ were obtained from the slope of the regression curve. The value of the $K_{SV}$ was $7.7x10^3$ $M^{-1}$ with a 99 % confidence level and the value for $K_q$ was $7.7x10^{11}$. As the $K_q$ value was larger than the maximal dynamic quenching constant in water ($2\times10^{10}$ $M^{-1}$ $s^{-1}$) it was confirmed that mv3glc effectively quenched the intrinsic fluorescence of grape seed 11SGb by the static mechanism predominantly caused by the formation of complexes. Similar quenching mechanism has been reported for the interaction between cyanidin 3-glcucoside and soybean 11S globulin (Chen et al., 2019; Ren et al., 2019; Dumitrascu, Stănciuc, Grigore-Gurgu, & Aprodu, 2020). Thus, the static binding constant ($K_S$) and binding sites numbers ($n$) were calculated from Stern-Volmer Eq. (3) by plotting the log $(F_0-F)/F$ versus log [mv3glc], which is showed in Fig. 2C. With a 99 % confidence level, the value for the static quenching constant $K_S$ for the interaction between mv3glc and grape seed 11SGb was $8.5x10^4$ $M^{-1}$ and the binding sites, $n$=1.3. These values were consistent with the affinity constants values and binding sites described for complexes between other proteins from vegetal (soy 11SGb) or animal origin (casein) with anthocyanin compounds, most of them in the order of $10^4$ $M^{-1}$ (Chen et al., 2019; Li et al., 2020).

### 3.3. Effect of grape seed 11SGb on mv3glc colour by differential tristimulus colorimetry

Table 1 shows the influence of increasing concentrations of grape seed globulins (1.5, 2.5, and 5.0 mg/ml) on the CIELAB colour parameters (L*, a*, b*, b*, $C^*_{ab}$, $h_{ab}$) of mv3glc solutions ($10^{-4}$ M), assessed in 0.2 M citrate buffer (12 % ethanol at pH 3.5). As

observed, the increasing additions of the 11SGb extract resulted in a slight decrease of lightness (L*) simultaneous to an increase of the chroma ($C^*_{ab}$) values, which mean that mv3glc solutions became progressively darker and with more vivid colour at the protein levels tested. These colorimetric effects reflect the shift of the anthocyanin equilibrium toward more coloured forms in the presence of 11SGb suggesting a preferential binding between such as grape seed proteins and the flavylium cation under simulated conditions similar to those found in wines (12 % ethanol and pH 3.5). As well, a slight decrease of the hue ($h_{ab}$) toward more negative values indicates that the blue component of colour tended to increase in solutions, that is, mv3glc exhibited a more red-bluish tonality in the presence of grape seed 11SGb. The slight positive changes observed in all the individual colour parameters were in accordance with the gradual increases of the Total Colour (E) of solutions (from 57 to 60 CIELAB u.), indicating that grape seed 11SGb produced a global intensification of the mv3glc colour. Moreover, the ability of grape seed globulins to modulate the colour characteristics of mv3glc seems to be significantly ($p$<0.05) correlated with its concentration since the higher protein level tested, the significant greater colour effects. However, the absolute differences in lightness, chroma and hue ($\Delta L^*$, $\Delta C^*_{ab}$ and $\Delta h_{ab}$) calculated between the 11SGb-mv3glc solutions at the highest protein level (5 mg/ml) respect to the mv3glc control solution (Table S1) denote that the quantitative and qualitative colour changes produced were small ($\Delta L^*$ = -2.4, $\Delta C^*_{ab}$ = +1.7, and $\Delta h_{ab}$= -1 CIELAB u., respectively).

Thus, to establish whether the slight changes observed in the individual CIELAB parameters were visually relevant, the colour differences ($\Delta E^*_{ab}$) between mv3glc solutions and the same solutions containing increasing concentrations of grape seed 11SGb were calculated. Furthermore, by comparing the relative contributions of lightness (%ΔL), chroma (%ΔC) and hue (%ΔH) that make up each colour difference ($\Delta E^*_{ab}$) was

418 possible to assess which colour attribute was most influenced according to the protein
419 concentration. As observed in Fig. 3, the $\Delta E^*_{ab}$ values tended to be higher as the
420 concentration of grape seed globulins increased in the mv3glc solutions suggesting that
421 the colour effect becomes more noticeable depending on the protein content. Also, it was
422 confirmed that the colour enhancement was mostly due to quantitative changes (%ΔL=
423 52-60 % and %ΔC=33-35 % at 5 mg/ml of protein) and to a lesser extent to qualitative
424 changes (%ΔH =7-13 % at 5 mg/ml of protein). However, the highest $\Delta E^*_{ab}$ values
425 observed at 2.5 and 5 mg/ml of protein ranged from 2.5 to 3.5 CIELAB u., which are
426 considered values close to the visual threshold to clearly perceive colour differences by
427 average non-trained observers, according to Martínez, Melgosa, Pérez, Hita, &
428 Negueruela (2001). Thus, the magnitude of the colour changes observed both in the
429 individual parameters and on the colour differences was slightly visually relevant, and
430 comparatively less notable than the colour impact reported for other compounds (as
431 certain phenolic copigments) when tested in similar conditions (Gordillo et al., 2012;
432 Gordillo et al., 2015; Rivero et al., 2022). These findings encourage developing further
433 and new investigations to better optimize the potential technological use of grape seed
434 globulins as colour protecting agents in wines or in the food industry.

435 **3.4. Guided-docking study and analysis between grape seed 11SGb and mv3glc**

436 Fluorescence quenching and colorimetric studies provided evidence of the formation of
437 a grape seed protein-wine anthocyanin complex resulting in the protection of the
438 flavylium cation against hydration reaction a pH 3.5 and in positive effects on mv3glc
439 colour. With the aim of supporting from a molecular point of view the experimental
440 interactions observed, computational studies were developed. In particular, a guided-
441 docking study was carried out between one of the grape seed 11SGb monomer identified
442 by mass spectrometry (F6HZK3, 60 kDa) in our previous study (Chamizo et al., 2022)

443 and mv3glc in order to improve the accuracy in the binding affinity prediction of the
444 interaction between grape seed proteins and wine anthocyanins.
445 For this purpose, this new docking study was carried out selecting specifically the major
446 hydrophobic region of the protein monomer (60 kDa) determined in our previous
447 computational results (Chamizo et al., 2022), as the most susceptible protein site to
448 interact with mv3glc.
449 Nine possible ligand conformations in the major hydrophobic protein environment were
450 obtained after each run in the AutoDock Vina software and the lowest energy
451 conformation (-6.8 Kcal/mol) was chosen as the most favourable conformation in the
452 binding site. This conformation is illustrated in Fig. 4A which shows the most favourable
453 specific binding site of the 11SGb monomer with the mv3gcl into the major hydrophobic
454 region of the protein (indicated in orange). As well, the binding model was represented
455 in two dimensions in Fig. 4B where the interactions established between the protein and
456 mv3glc are shown. As observed, the amino acids involved in the interaction were mainly
457 Gly 151 and Gln 133, which establish hydrogen bond with the hydroxyl groups of the
458 glucose and the A ring of mv3glc, respectively. Moreover, the aromatic amino acid
459 Phe153 establishes π-π and alkyl hydrophobic interactions with both B and C rings of
460 mv3glc (binding distance about 4.1 and 4.4 Å). Other interactions such as Van der Waals
461 forces also are present in the protein-ligand interaction. Such as hydrophobic interactions
462 are similar to those widely described for different copigmentation associations between
463 wine copigments and anthocyanins, according to Trouillas et al., (2016). Our results also
464 agreed with those of protein-anthocyanin interactions involving 11SGb from other
465 vegetal sources (soy proteins), which have confirmed that aromatic amino acids such as
466 tryptophan are responsible of the non-covalent binding with the pigment (Dumitriascu et
467 al., 2020).

### 3.5. Stability analysis of the grape seed 11SGb-mv3glc complex by molecular dynamics simulation

The stability of the binding conformation and mode for the 11SGb-mv3glc complex was assessed by MD simulation during 10 ns in a solvated and equilibrated system. In addition, the stability of the 11SGb and the mv3glc were individually assessed for comparative purposes. One of the most commonly used parameters in MD to analyse the conformational stability of a protein-ligand complex is the RMSD parameter, in this case applied to C-α atoms of the protein backbone. In general, low values of RMSD with constant fluctuations during MD simulation time indicate that the system is stable while high RMSD values are typical of unstable systems (Wu, et al., 2021; Zhao, et al., 2022).

The plot of RMSD values during the MD simulation time for the three systems (11SGb, mv3glc, and the 11SGb-mv3glc complex) is shown in Fig. 5A. The RMSD values obtained for the 11SGb-mv3glc complex ranged from 0.20 to 0.50 nm showing small fluctuations. In the case of the 11SGb alone (red line), the values of RMSD ranged from 0.2 to 0.65 nm and for the mv3glc (blue line) between 0.10 and 0.20 nm. Thus, the 11SGb-mv3glc complex exhibited lower RMSD values than the protein alone (11SGb) suggesting that the binding of the mv3glc to the grape seed protein improved the conformational stability of the system. Furthermore, the lowest RMSD values found for the mv3glc alone indicate that the pigment is stable in the protein-binding site during the simulation. These conformational changes can be better visualized in Fig. 1S, and the Fig. 5B, where the protein-pigment interaction is showed with more detail during the last period of the MD simulation (7, 8, 9, and 10 ns).

The number of hydrogen bonds formed by the 11SGb with mv3glc was calculated and plotted versus MD simulation time (Fig. 5C). Results showed that the protein established between 0 and three hydrogen bonds with the pigment during the MD simulation, with

493 an average value of two hydrogen bonds. The analysis of MD simulation results using the
494 Discovery studio software showed that the main amino acids involved in the interaction
495 with hydroxyl groups of the A ring of mv3glc trough hydrogen bonds were Gln 133 and
496 Glu 82, which agreed with the docking results for the former. These findings suggest that
497 Gln 133 residue of the grape seed 11SGb could have a key role in the stabilisation of
498 mv3gcl. Such as amino acid residues have also been reported to participate the interaction
499 of heated soy proteins with anthocyanins from cornelian cherry fruits (Dumitrascu et al.,
500 2020).

501 **CONCLUSIONS**

502 Fluorescence quenching in combination with colorimetric studies confirmed that the
503 grape seed 11SGb interacts with mv3gcl through static binding mechanism contributing
504 to positively modulate the colour characteristics of the major grape and wine anthocyanin.
505 The colorimetric benefits achieved (mainly quantitative and to a lesser extent qualitative)
506 were dependent on the protein concentration and slightly visually discernible. The
507 formation of a stable 11SGb-mv3glc complex in the most hydrophobic site of the protein
508 driven by hydrogen bounds and Van der Walls forces was suggested by the molecular
509 modelling studies. Specifically, the acidic subunit of 11SGb monomer mainly involved
510 in the interaction was found as a one of the major polypeptide of the grape seed globulin
511 fraction, which could be of particular interest for colour protection applications in the
512 food industry and especially in winemaking sector.

513

514 **Acknowledgments**

515 Authors thank the assistance of the technical staff of Biology Service (SGI, Universidad
516 de Sevilla, Spain) and the Scientific Computation Center of Andalusia (CICA) for the
517 computing services they provided.

**Funding sources**

This research was financially supported by the Ministerio de Economía y Competitividad, Spain, Gobierno de España (Project PID2021-127126OB-C2 and FPI grant PRE2018-087184). E. Manjón thanks Junta de Castilla y León-FEDER Programme (Project Ref. SA0093P20) for her postdoctoral contract.

**Conflict of interest statement**

Authors declare no conflict of interest.

**References**

Baca-Bocanegra, B., Nogales-Bueno, J., Hernández-Hierro, J. M., & Heredia, F. J. (2021). Optimization of Protein Extraction of Oenological Interest from Grape Seed Meal Using Design of Experiments and Response Surface Methodology. *Foods*, *10*(1), 79. https://doi.org/10.3390/foods10010079

Boulton, R. (2001). The copigmentation of anthocyanins and its role in the color of red wine: A critical review. *American journal of enology and viticulture*, *52*(2), 67-87.

Casanova, F., Chapeau, A. L., Hamona, P., Carvalho, A. F., Croguennec, T., & Bouhallab, S. (2018). pH and ionic strength-dependent interaction between cyanidin-3-O-glucoside and sodium caseinate. *Food Chemistry*, *267*, 57-58. http://dx.doi.org/10.1016/j.foodchem.2017.06.081.

Chamizo-González, F., Gordillo, B., & Heredia, F. J. (2021). Elucidation of the 3D structure of grape seed 7S globulin and its interaction with malvidin 3-glucoside: A molecular modelling approach. *Food Chemistry*, *347*, 129014. https://doi.org/10.1016/j.foodchem.2021.129014

Chamizo-González, F., Heredia, F. J., Rodríguez-Pulido, F. J., González-Miret, M. L., & Gordillo, B. (2022). Proteomic and computational characterisation of 11S globulins

543 from grape seed flour by-product and its interaction with malvidin 3-glucoside by
544 molecular docking. *Food Chemistry*, *386*, 132842.
545 https://doi.org/10.1016/j.foodchem.2022.132842
546 Chen, Z., Wang, C., Gao, X., Chen,Y., Santhanam, R. K., Wang, C., Xu, L., & Chen, H.
547 (2019). Interaction characterization of preheated soy protein isolate with cyanidin-
548 3-O-glucoside and their effects on the stability of black soybean seed coat
549 anthocyanins extracts. *Food Chemistry*, *271*, 266- 273.
550 https://doi.org/10.1016/j.foodchem.2018.07.170
551 CIE. Technical Report Colorimetry; Commission Internationale de l'Eclairage Central
552 Bureau: Vienna, Austria, 2004.
553 Delgado-Vargas, F., Jiménez, A. R., & Paredes-López, O. (2000). Natural pigments:
554 carotenoids, anthocyanins, and betalains-characteristics, biosynthesis, processing,
555 and stability. *Critical reviews in food science and nutrition*, *40*(3), 173-289.
556 https://doi.org/10.1080/10408690091189257
557 Dumitrascu, L., Stănciuc, N., Grigore-Gurgu, L., & Aprodu, I. (2020). Investigation on
558 the interaction of heated soy proteins with anthocyanins from cornelian cherry fruits.
559 *Spectrochimica Acta Part A: Molecular and Biomolecular spectrometry*, *231*,
560 118114. https://doi.org/10.1016/j.saa.2020.118114
561 Escribano-Bailón, M. T., & Santos-Buelga, C. (2012). Anthocyanin copigmentation-
562 evaluation, mechanisms and implications for the colour of red wines. *Current*
563 *Organic Chemistry*, *16*(6), 715-723. https://doi.org/10.2174/138527212799957977
564 Escribano-Bailón, M. T., Rivas-Gonzalo, J. C., & García-Estévez, I. (2019). Wine color
565 evolution and stability. In *Red wine technology*. A. Morata (Ed.). Elsevier, Academic
566 Press, 195-205. https://doi.org/10.1016/B978-0-12-814399-5.00013-X
567 Ferrer-Gallego, R., Brás, N. F., García-Estévez, I., Mateus, N., Rivas-Gonzalo, J. C., de

568 Freitas, V., & Escribano-Bailón, M. T. (2016). Effect of flavonols on wine
569 astringency and their interaction with human saliva. *Food Chemistry*, 209, 358-364.
570 http://dx.doi.org/10.1016/j.foodchem.2016.04.091
571 Fernandes, A., Raposo, F., Evtuguin, D. V., Fonseca, F., Ferreira-da-Silva, F., Mateus,
572 N., & de Freitas, V. (2021). Grape pectic polysaccharides stabilization of
573 anthocyanins red colour: Mechanistic insights. *Carbohydrate Polymers, 255*,
574 117432. https://doi.org/10.1016/j.carbpol.2020.117432
575 Martínez, J. A., Melgosa, M., Pérez, M. M., Hita, E., & Negueruela, A. I. (2001). Visual
576 and instrumental color evaluation in red wines. *Food Science and Technology*
577 *International*, *7*, 439-444. https://doi.org/10.1106/VFAT-5REN-1WK2-5JGQ
578 Fitzjohn, P. W., & Bates, P. A. (2003). Guided docking: first step to locate potential
579 binding sites. Proteins. *Structure, Function, and Bioinformatics*, *52*(1), 28-32.
580 https://doi.org/10.1002/prot.10380
581 Gordillo, B., Chamizo-González, F., González-Miret, M. L., & Heredia, F. J. (2021).
582 Impact of alternative protein fining agents on the phenolic composition and color of
583 Syrah red wines from warm climate. *Food Chemistry*, *342*, 128297.
584 https://doi.org/10.1016/j.foodchem.2020.128297
585 Gordillo, B., Rodríguez-Pulido, F. J., González-Miret, M. L., Quijada-Morín, N., Rivas-
586 Gonzalo, J. C., García-Estévez, I., & Escribano-Bailón, M. T. (2015). Application
587 of differential colorimetry to evaluate anthocyanin-flavonol-flavanol ternary
588 copigmentation interactions in model solutions. *Journal of Agricultural and Food*
589 *Chemistry*, *63*(35), 7645-7653. https://doi.org/10.1021/acs.jafc.5b00181
590 Granato, T. M., Ferranti, P., Iametti, S., & Bonomi, F. (2018). Affinity and selectivity of
591 plant proteins for red wine components relevant to color and aroma traits. *Food*
592 *Chemistry*, *256*, 235-243. https://doi.org/10.1016/j.foodchem.2018.02.085

He, J., & Giusti, M. M. (2010). Anthocyanins: natural colorants with health-promoting properties. *Annual Review of Food Science and Technology*, *1*(1), 163-187. https://doi.org/10.1146/annurev.food.080708.100754

Heredia, F. J.; Álvarez, C.; González-Miret, M.L.; & Ramírez, A. CromaLab, análisis de color. Registro General de la Propiedad Intelectual, 2004.

Lakowicz, J. R. (2013). *Principles of fluorescence spectroscopy*. Springer science & business media.

Li, T., Wang, L., Chen, Z., Zhang, X., & Zhu, Z. (2020). Functional properties and structural changes of rice proteins with anthocyanins complexation. *Food Chemistry*, *331*, 127336. https://doi.org/https://doi.org/10.1016/j.foodchem.2020.127336.

Marangon, M., Vincenzi, S., & Curioni, A. (2019). Wine fining with plant proteins. *Molecules*, *24*(11), 2186. https://doi.org/10.3390/molecules24112186

Martínez, J. A., Melgosa, M., Pérez, M. M., Hita, E., & Negueruela, A. I. (2001). Visual and instrumental color evaluation in red wines. *Food Science and Technology International*, *7*, 439-444. DOI: 10.1106/VFAT-5REN-1WK2-5JGQ

Mora-Garrido, A. B., Cejudo-Bastante, M. J., Heredia, F. J., & Escudero-Gilete, M. L. (2022). Revalorization of residues from the industrial exhaustion of grape by-products. *LWT-Food Science and Technology*, *156*, 113057. https://doi.org/10.1016/j.lwt.2021.113057

Mujoo, R., Trinh, D. T., & Ng, P. K. (2003). Characterization of storage proteins in different soybean varieties and their relationship to tofu yield and texture. *Food chemistry*, *82*(2), 265-273. https://doi.org/10.1016/S0308-8146(02)00547-2

Pettersen, E. F., Goddard, T. D., Huang, C. C., Couch, G. S., Greenblatt, D. M., Meng, E. C., & Ferrin, T. E. (2004). UCSF Chimera--a visualization system for exploratory research and analysis. *Journal of Computational Chemistry*, *25*(13), 1605-1612.

https://doi.org/10.1002/jcc.20084

Pina, F., Oliveira, J., & de Freitas, V. (2015). Anthocyanins and derivatives are more than flavylium cations. *Tetrahedron*, *71*(20), 3107-3114. https://doi.org/10.1016/j.tet.2014.09.051

Rawel, H. M., Meidtner, K., & Kroll, J. (2005). Binding of selected phenolic compounds to proteins. *Journal of Agricultural and Food Chemistry*, *53*(10), 4228-4235. https://doi.org/10.1021/jf0480290

Ren, C., Xiong, W., & Li, B. (2019). Binding interaction between β-conglycinin/glycinin and cyanidin-3-O-glucoside in acidic media assessed by multi-spectroscopic and thermodynamic techniques. *International Journal of Biological Macromolecules*, *137*, 366-373. https://doi.org/10.1016/j.ijbiomac.2019.07.004

Sacchi, K. L., Bisson, L. F., & Adams, D. O. (2005). A review of the effect of winemaking techniques on phenolic extraction in red wines. *American Journal of Enology and Viticulture*, *56*(3), 197-206.

Soto Vázquez, E., Río Segade, S., & Orriols Fernández, I. (2010). Effect of the winemaking technique on phenolic composition and chromatic characteristics in young red wines. *European Food Research and Technology*, *231*(5), 789-802. https://doi.org/10.1007/s00217-010-1332-5

StatSoft Inc. STATISTICA (data analysis software system), v 8; StatSoft Inc.: Tulsa, OK, 2007

Trott, O., & Olson, A. J. (2010). AutoDock Vina: improving the speed and accuracy of docking with a new scoring function, efficient optimization, and multithreading. *Journal of Computational Chemistry*, *31*(2), 455-461. https://doi.org/10.1002/jcc.21334

Trouillas, P., Sancho-García, J. C., De Freitas, V., Gierschner, J., Otyepka, M., &

643 Dangles, O. (2016). Stabilizing and modulating color by copigmentation: Insights
644 from theory and experiment. *Chemical Reviews*, *116*(9), 4937-4982.
645 https://doi.org/10.1021/acs.chemrev.5b00507
646 Vanommeslaeghe, K., Hatcher, E., Acharya, C., Kundu, S., Zhong, S., Shim, J., Darian,
647 E., Guvench, O., Lopes, P., & Vorobyov, I. (2010). CHARMM general force field:
648 A force field for drug- like molecules compatible with the CHARMM all- atom
649 additive biological force fields. *Journal of Computational Chemistry*, *31*(4), 671-
650 690. https://doi.org/10.1002/jcc.21367
651 Wei, J., Xu, D., Yang, J., Zhang, X., Mu, T., & Wang, Q. (2018). Analysis of the
652 interaction mechanism of Anthocyanins (Aronia melanocarpa Elliot) with β-casein.
653 *Food Hydrocolloids*, *84*, 276-281. https://doi.org/10.1016/j.foodhyd.2018.06.011
654 Wu, D., Tang, L., Duan, R., Hu, X., Geng, F., Zhang, Y., & Li, H. (2021). Interaction
655 mechanisms and structure-affinity relationships between hyperoside and soybean β-
656 conglycinin and glycinin. *Food Chemistry*, *347*, 129052.
657 https://doi.org/10.1016/j.foodchem.2021.129052
658 Zhao, G., Zhu, L., Yin, P., Liu, J., Pan, Y., Wang, S., & Liu, X. (2022). Mechanism of
659 interactions between soyasaponins and soybean 7S/11S proteins. *Food Chemistry*,
660 *368*, 130857. https://doi.org/10.1016/j.foodchem.2021.130857
661 Zheng, J., Zheng, X., Zhao, L., Yi, J., & Cai, S. (2021). Effects and interaction mechanism
662 of soybean 7S and 11S globulins on anthocyanin stability and antioxidant activity
663 during in vitro simulated digestion. *Current Research in Food Science*, *4*, 543-550.
664 https://doi.org/10.1016/j.crfs.2021.08.003
665

666 **FIGURE CAPTIONS**

**Fig. 1.** SDS-PAGE electrophoresis carried out for the quantification of the polypeptides of 11S grape seed globulin. Lanes 1-5 show the protein standard BSA calibration curve at increasing levels (12.5, 25, 50, 100, and 200 μg/ml). Lane 6 corresponds to the molecular weight marker (20-200 kDa) and lanes 7-10 correspond to the bands of the 11S globulin protein replicates (n=4) under reduced conditions.

**Fig. 2.** A) Mean fluorescence emission spectra of the 11SGb (50 μM) in the presence of increasing concentrations of mv3glc (0-100 μM), at pH 3.5 and 25 °C. B) Stern-Volmer plot for the quenching of 11SGb (50 μM) at increasing concentrations of mv3glc (0-100 μM), at pH 3.5 and 25 °C. C) Double-logarithmic regression plot of 11SGb (50 μM) at increasing concentrations of mv3glc (0-100 μM), at pH 3.5 and 25 °C.

**Fig. 3.** Colour differences ($\Delta E^*_{ab}$), with the relative contribution of lightness, chroma, and hue (%ΔL, %ΔC, %ΔH), between mv3glc solutions ($10^{-4}$ M) and the same solutions containing increasing concentrations of the11SGb extract (1.5, 2.5, and 5.0 mg/ml).

**Fig. 4**. A) 3D conformation of the 11SGb from grape seed interacting with mv3glc, elaborated by a homology model. Hydrophilic regions of the 11SGb are shown in blue and hydrophobic regions in orange. B) 2D illustration of the interaction of mv3glc with 11SGb residues showing the main interactions in different colours. Abbreviations: Proline (Pro), Histidine (His), Glycine (Gly), Methionine (Met), Glutamine (Gln) and Phenylalamine (Phe).

**Fig. 5**. A) RMSD of 11SGb backbone Cα atoms in complexation with mv3glc (black), 11SGb backbone Cα atoms (red) and mv3glc (blue). B) Stability of mv3glc at the 11SGb -binding site during the last molecular dynamics period (7-10 ns). C) Hydrogen bonding profile of 11SGb in complex with mv3glc.

**Declaration of interests**

☐The authors declare that they have no known competing financial interests or personal relationships that could have appeared to influence the work reported in this paper.

☒The authors declare the following financial interests/personal relationships which may be considered as potential competing interests:

Francisco J. Heredia reports financial support was provided by Ministerio de Economía y Competitividad, Spain, Gobierno de España. Elvira Manjon reports financial support was provided by Junta de Castilla y León-FEDER Programme.

Credit Author Statement

Francisco Chamizo: Investigation

Belén Gordillo: Investigation, Writing - Original Draft

Ignacio García Estévez:  Investigation, Writing - Original Draft

Elvira Manjón: Investigation

M.T. Escribano-Bailón: Conceptualization, Supervision

Francisco J. Heredia: Conceptualization, Supervision

M. Lourdes González-Miret: Conceptualization, Writing revision

Table 1

**Table 1.** Changes on the colour characteristics of the mv3glc model solutions ($10^{-4}$ M, n=3) after the addition of increasing concentrations of the11SGb extract (1.5, 2.5, and 5.0 mg/ml).

| | **Mv3glc** | **Mv3glc + 11SGb** | | |
|---|---|---|---|---|
| | **$10^{-4}$ M** | **1.5 mg/ml** | **2.5 mg/ml** | **5.0 mg/ml** |
| L* | 69.40±0.30 $^{a}$ | 68.10±0.13 $^{b}$ | 67.77±0.01 $^{bc}$ | 67.22±0.29 $^{c}$ |
| a* | 48.80±0.39 $^{a}$ | 49.25±0.02 $^{a}$ | 50.69±0.02 $^{b}$ | 50.54±0.14 $^{b}$ |
| b* | - 5.14±0.07 $^{a}$ | - 4.03±0.05 $^{b}$ | - 4.46±0.05 $^{c}$ | - 4.42±0.05 $^{c}$ |
| $C_{ab}$ | 49.10±0.38 $^{a}$ | 49.42±0.01 $^{a}$ | 50.88±0.02 $^{b}$ | 50.73±0.15 $^{b}$ |
| $h_{ab}$ | - 6.02±0.12 $^{a}$ | - 4.68±0.06 $^{b}$ | - 5.02±0.06 $^{c}$ | - 5.00±0.04 $^{c}$ |
| E (Total Colour) | 57.83 | 58.85 | 60.22 | 60.30 |

Different letters in the same row indicate significant differences ($p$<0.05; Tukey's test) between Mv3glc solutions and the same solutions containing increasing concentrations of 11SGb.

Figure 1.

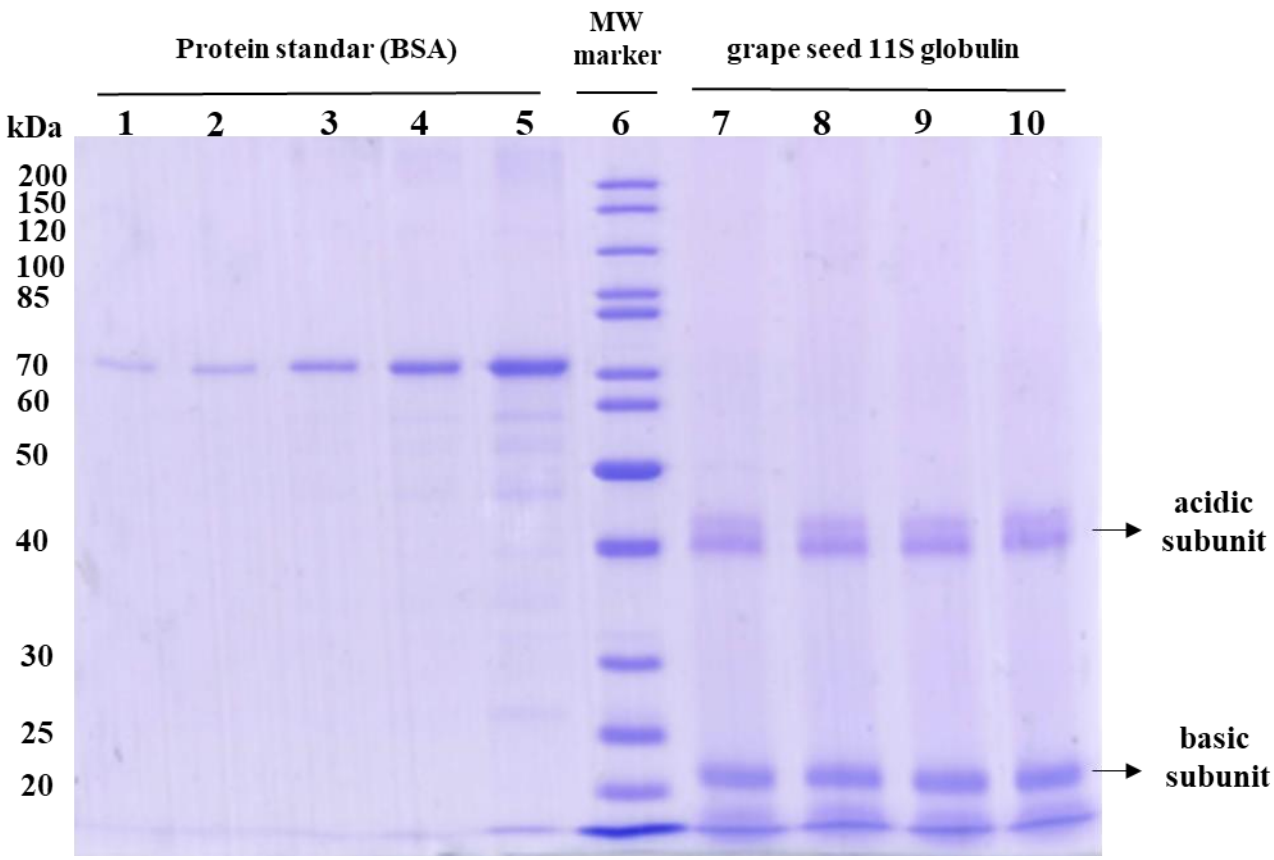

Figure 2.

A)

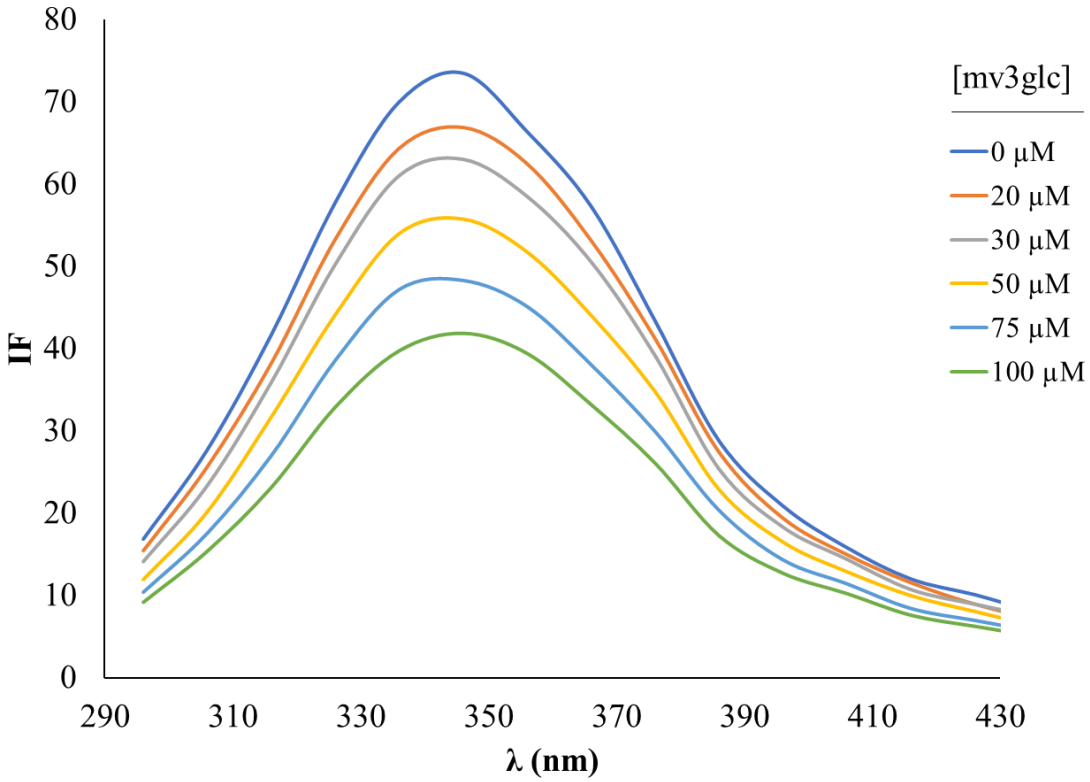


B)

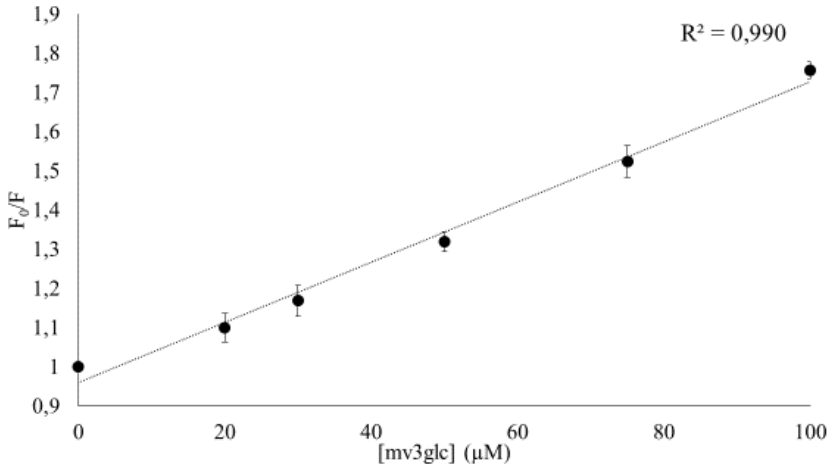

C)

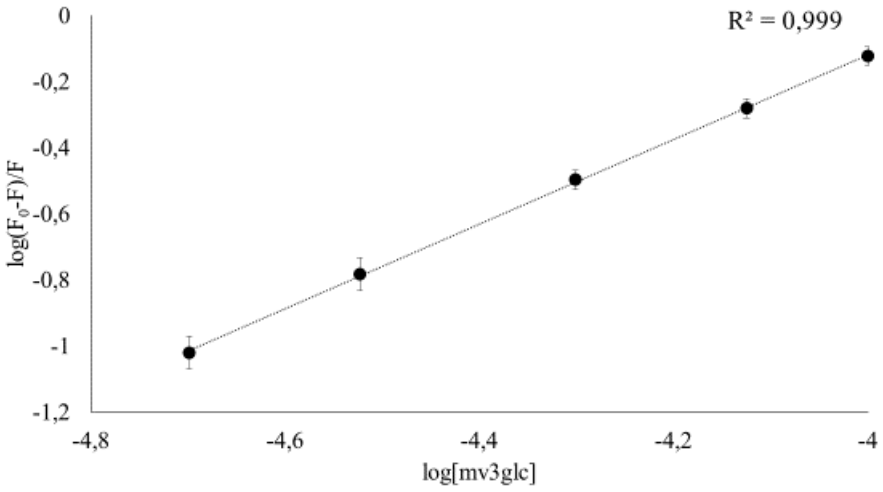

Figure 3.

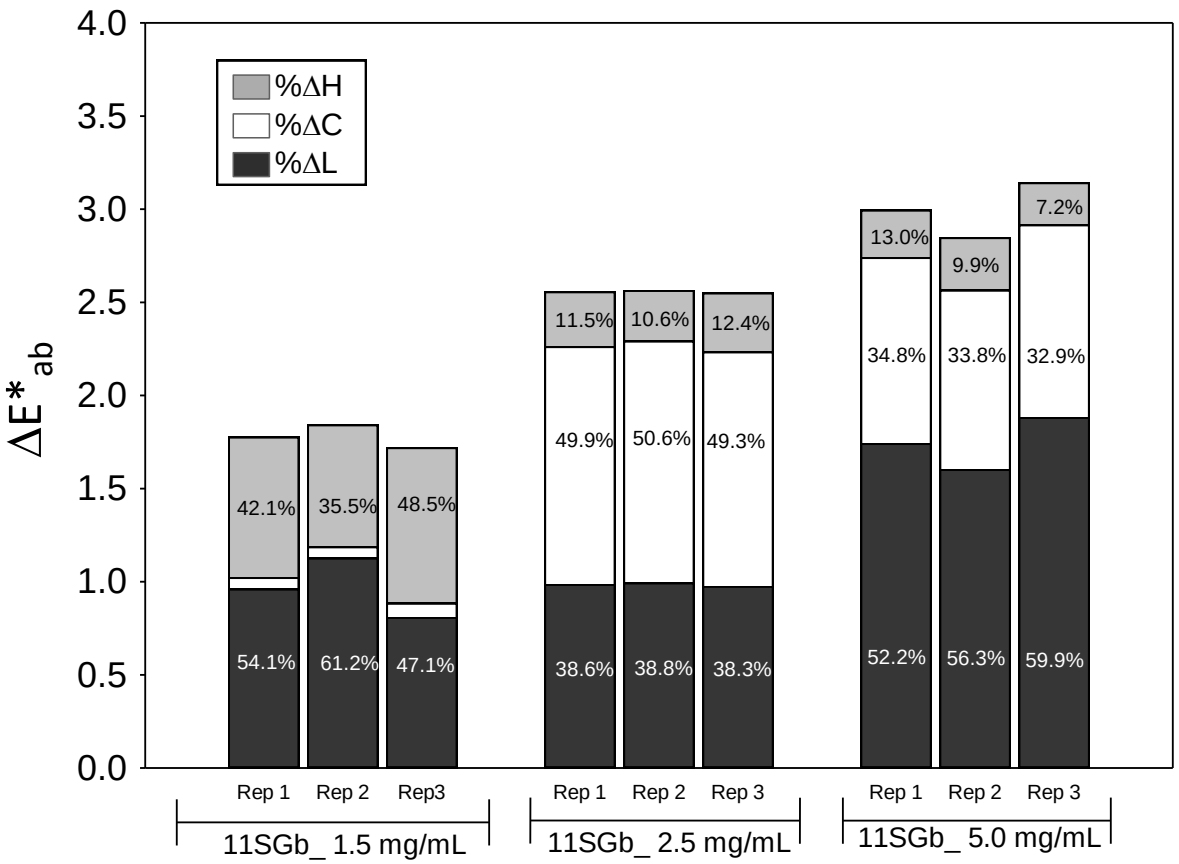

Figure 4

A)

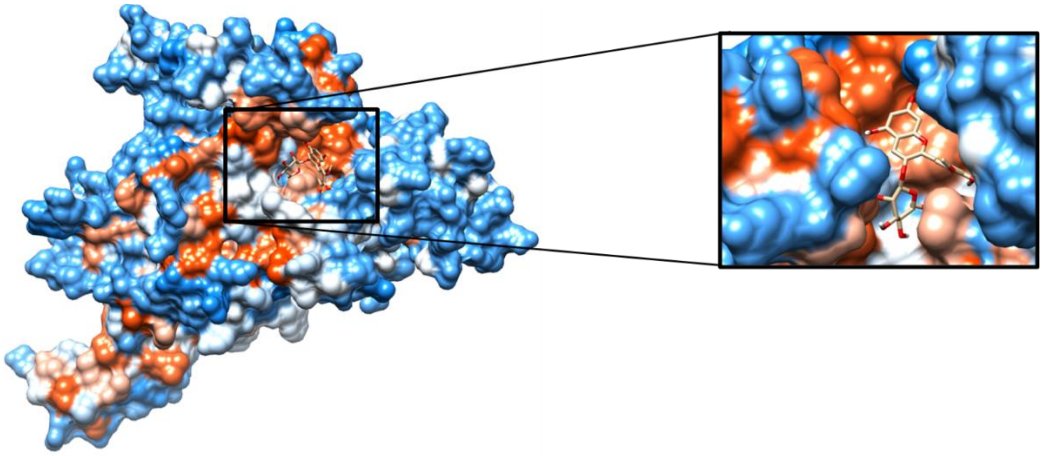

B)

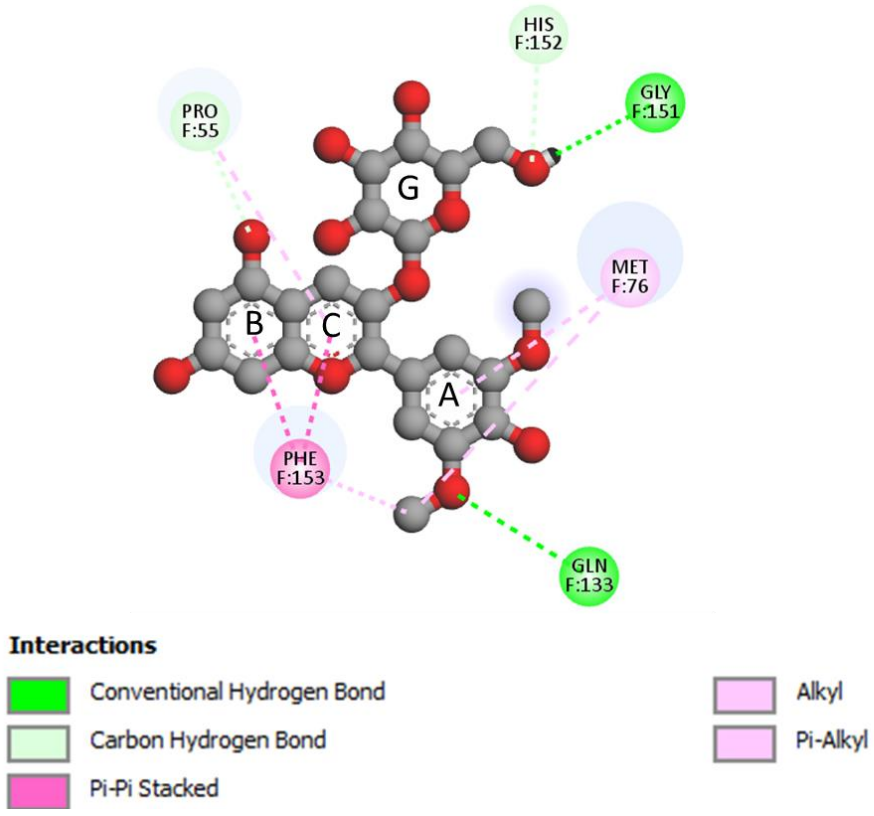

Figure 5.

A)

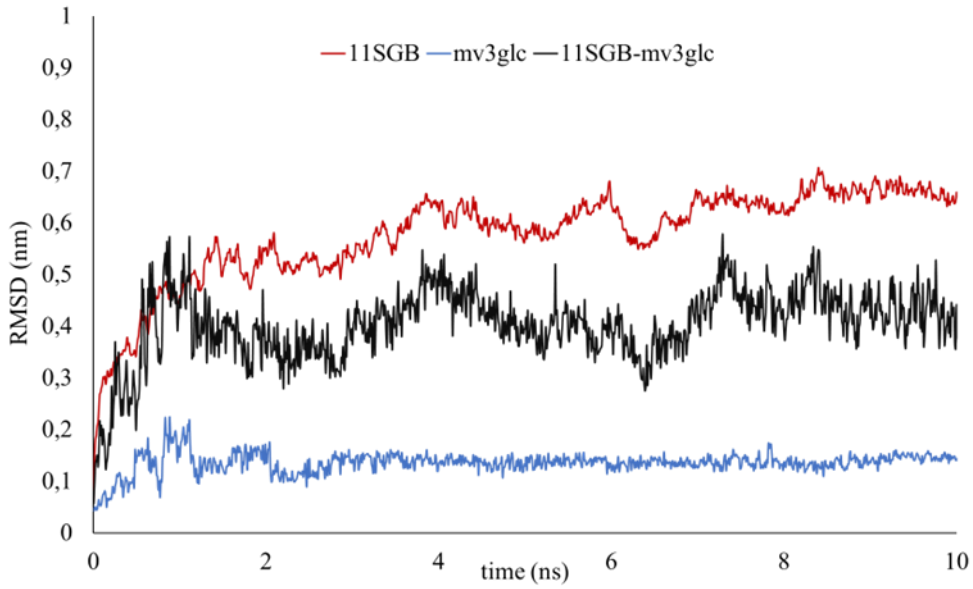


B)

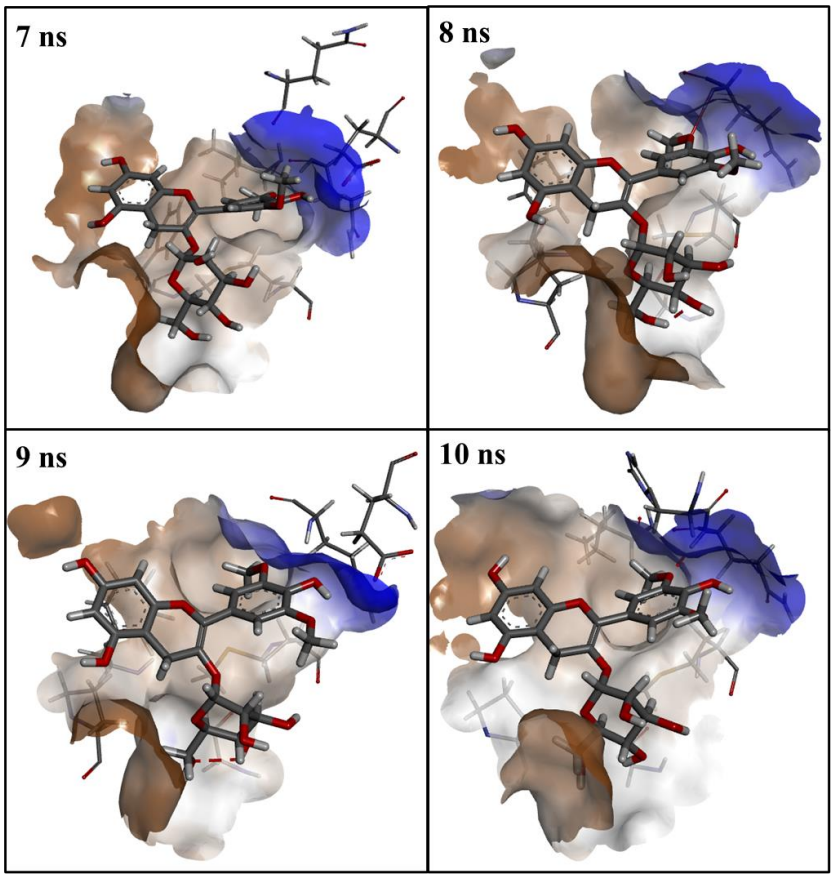

C)

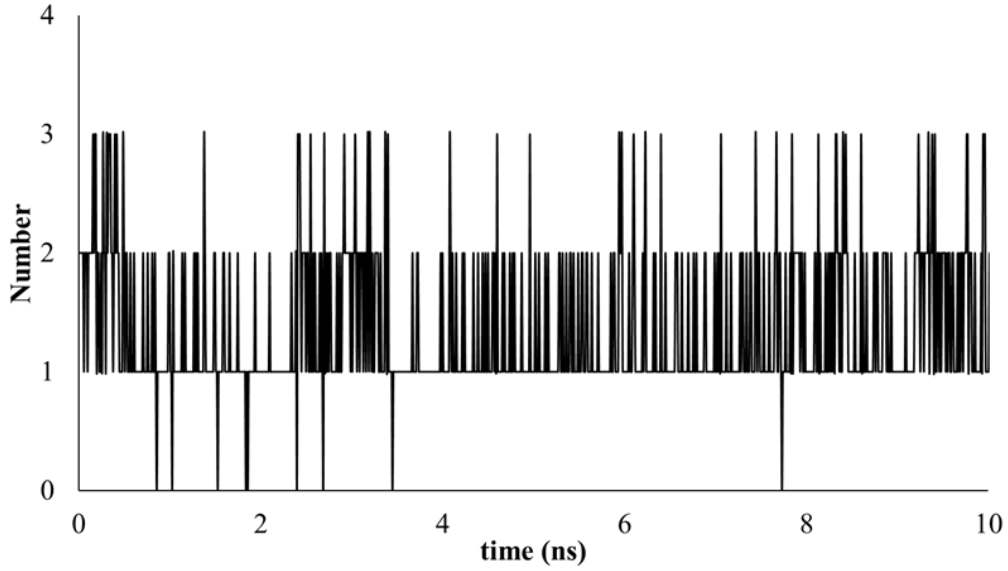

**Table S1.** Absolute colour, lightness, chroma, and hue differences ($\Delta E^*_{ab}$, $\Delta L^*$, $\Delta C^*_{ab}$, $\Delta h_{ab}$) calculated between the 11SGb-mv3glc solutions with respect to the mv3gcl control solution ($10^{-4}$ M, n=3), at increasing protein concentration (1.5, 2.5, and 5.0 mg/ml).

| | **[Mv3glc + 11SGb]- Mv 3 glc** | | |
|---|---|---|---|
| | **1.5 mg/ml** | **2.5 mg/ml** | **5.0 mg/ml** |
| $\Delta E^*_{ab}$ | 1.78±0.06 [a] | 2.56±0.01[b] | 2.85±0.29[b] |
| $\Delta L^*$ | - 1.31±0.13[a] | - 1.59±0.01[a] | - 2.14±0.29[b] |
| $\Delta C^*_{ab}$ | + 0.34±0.01[a] | + 1.81±0.02[b] | + 1.66±0.15[b] |
| $\Delta h_{ab}$ | + 1.34±0.06[a] | + 1.00±0.06[b] | + 1.02±0.04[b] |

Different letters in the same row indicate significant differences ($p$<0.05, Tukey's test)

Figure S1

Click here to access/download;Supplementary Material;Chamizo_11SGbMv_Supp Material_FigS1.pptx

**Fig. 1S**. Dynamic molecular simulation

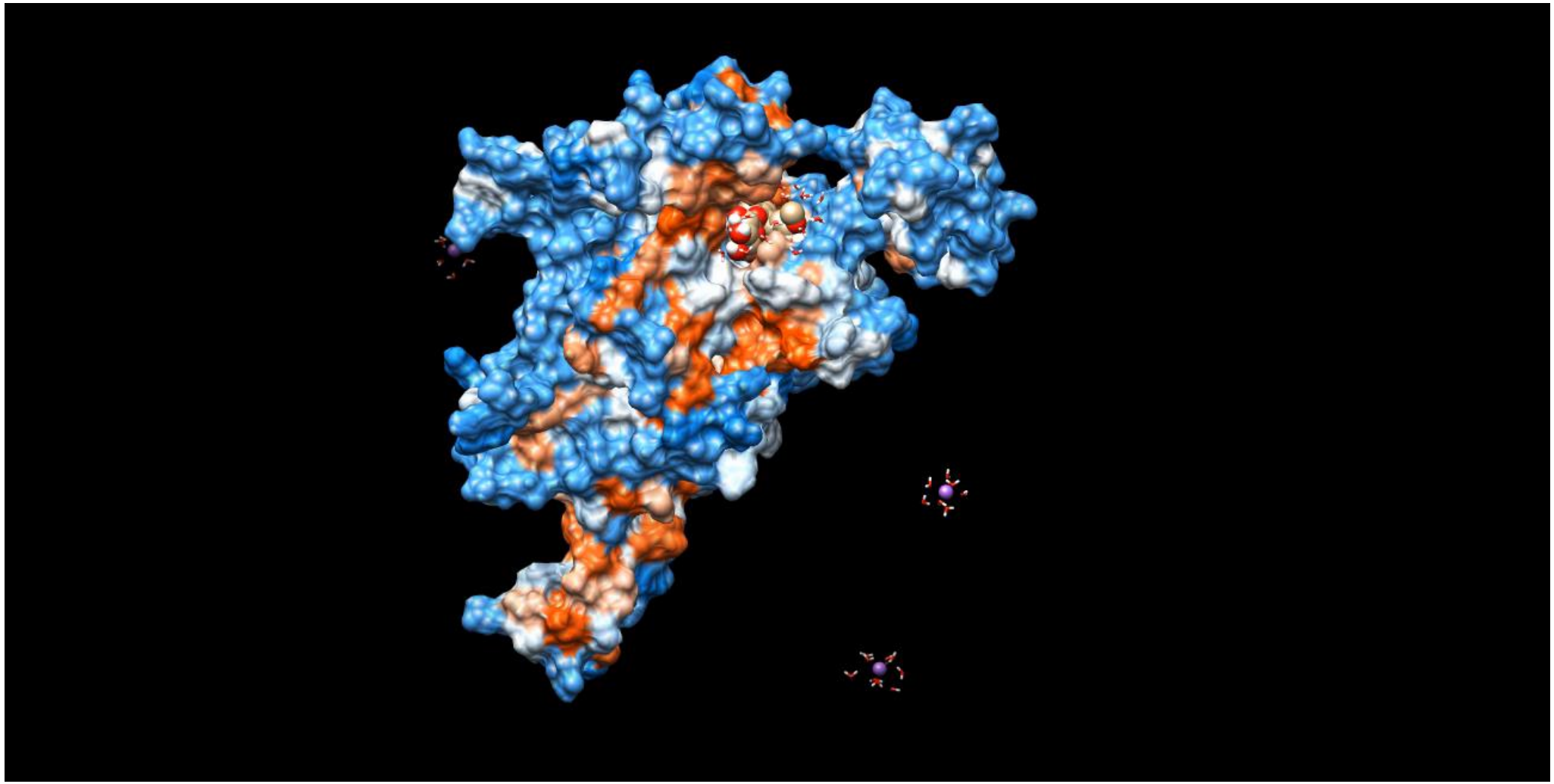

Figure S2. Absorption spectra (A.U.) of the mv3glc model solutions ($10^{-4}$ M) in the presence of increasing concentrations of the11SGb extract (0, 1.5, 2.5, and 5.0 mg/ml). The spectra of mv3glc solutions were corrected in the visible range by the absorbance spectra of 11SGb solutions at increasing concentrations.